Wheel Profile Analysis of 50 Tons Coal Wagon in South Sumatra Indonesia to Reduce Derailment Potential

Dwi Priyo Prayitno(✉) and Muhammad Akhsin Muflikhun

Mechanical and Industrial Engineering Department, Gadjah Mada University, Yogyakarta, Indonesia
dwipriyo2020@mail.ac.id, akhsin.muflikhun@ugm.ac.id

Abstract. The object of this research is the profile of the wheels of the 50 tons capacity coal transport train, the Babaranjang Train, which is operated by PT Kereta Api Indonesia (Persero), or PT KAI, in South Sumatra, Indonesia. The Babaranjang Train uses a wheel called as Roda Golongan DD, with a slope profile of 1:40. In this paper, it is proposed to use a more conical wheel profile to reduce the potential for derailment. Derailment, mainly caused by changes in the geometry of the wheel profile due to wear that occurs in the contact between wheel and rail surface. Research is to use rail vehicle dynamics analysis on wheel and rail contact using Universal Mechanism software. In this paper, a comparison will be made using the wheel profiles of 1:40, 1:20 and 1:10 on the Babaranjang Train. The result is that wheels with a tread profile slope of 1:20 show a 18.59% lower derailment potential than wheels with a tread profile slope of 1:40. The 1:10 wheel profile shows an even greater reduction in potential derailment than the 1:40 wheel profile, which is 40.80%. Replacing the 1:40 wheel profile with a more conical wheel profile will reduce PT KAI's financial losses due to the Babaranjang Train derailment.

Keywords: Wheel · Derailment · Profile

1 Introduction

Figure 1 is the track of the Babaranjang Train which transports 3000 Tons of coal in a trip from Tanjung Enim Baru Station to Tarahan Station (a). In several cases the wheel derailment of the Babaranjang Train wagon (b), was caused by changes in the geometry of the wheels and rails due to wear and having a track with lots of curves. The research is focused on the track between Prabumulih Station to Kotabumi Station which is identified as the track that has the most critical character. Currently, the Babaranjang Train uses a 1:40 wheel profile and in this study it is proposed to use a more conical wheel profile.

2 Materials and Method

2.1 Theory

In Fig. 2 shows a wheelset with conicity γ, wheel diameter D and the distance between the contact points of the wheels and the left and right rails is 2b. Wheelset passing

T. P. Syawitri et al. (Eds.): MEST 2022, AER 222, pp. 377–390, 2023.
https://doi.org/10.2991/978-94-6463-134-0_37

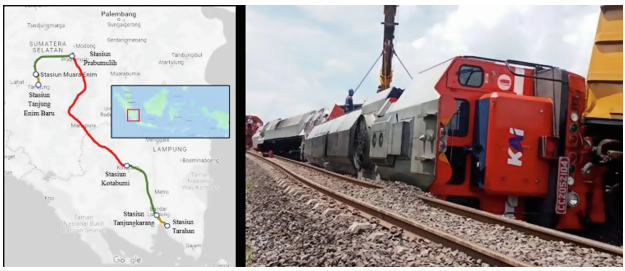

Fig. 1. Map of the track of Babaranjang Train (a) and the derailment (b). Source: https://koranmetronews.id/index.php/2021/12/11/kereta-api-babaranjang-dari-tarahan-menuju-tanjung-enim-tergelincir-di-emplasmen-penangiran/).

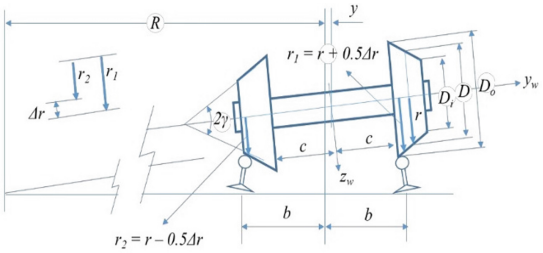

Fig. 2. Conical wheel set that rolls in curve track.

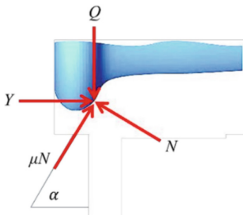

Fig. 3. Wheel and rail contact point.

through a track curve with radius R and make lateral displacements y. D_I is the wheel diameter on the inner curve track and D_o is the wheel diameter on the outer curve track. Wheel conicity γ provides information about wheel–rail interaction [1]:

(1) a high conicity value is suitable to counteract the centrifugal effects on curved track, but it generates a periodic movement on straight sections that can reduce riding comfort; and

(2) low conicity increases the ride quality, but on curved track it can cause the contact between the rail gauge and the wheel flange, producing excessive wear for both rail and wheel.

Running dynamics investigations will show that the difference in rolling radius $\Delta r = r2 - r1$ has a significant influence on the stability of the wheelset, while the difference in angle of contact or the elevation of the center of gravity are measures for how the

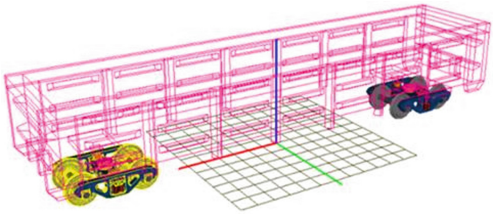

Fig. 4. Coal wagon modeling capacity of 50 tons.

mass is pushing the wheelset back to the central position while displaced [2]. For a rail vehicle to negotiate a curve, there must be a certain difference in the rolling radii of the two wheels on the wheelset. If this radii difference does not emerge, the contact point is located over the wheel flange, leading to major sliding and higher risk of derailment [3]. Therefore, wear on wheels will make radii difference not occur so to appear derailment potential.

One of the most used variables that represents the safety of railway transportation are the lateral and vertical forces that occurs due to wheel-rail contact (Fig. 3). The ratio between the lateral and vertical forces (Y/Q) is commonly used as an indication of the track quality and therefore vehicle safety in terms of its dynamic behavior [4]. The equation of the forces acting at the contact point of the wheel and rail is as follows:

$$\frac{Y}{Q} = \frac{\tan \alpha - \mu}{1 + \mu \tan \alpha} \tag{1}$$

Nadal limits the ratio (Y/Q) < 0.8 so that the wheelset does not cause derailment. This criterion is referred to by many researchers and practitioners in the railway industry, as well as in this study. By using a safety factor of 2.5 (in Indonesian railways), the maximum (Y/Q) ratio is 0.32 [5].

2.2 Methodology

This research was conducted in a simulation using Universal Mechanism software. Modeling of rail vehicles, consisting of body of wagon, bogie sets and wheelsets, is entirely made in the software. In the modeling, analytical validation is carried out to ensure that the model made is feasible and the simulation results are close to actual conditions. Validation using wagon specification data, includes the center of gravity that is not exactly on the centerline of the multi body system (MBS). In the multibody simulations a real mission profile of the vehicle is considered [6].

Modelling of body (Fig. 4), bolster bogie, suspension system (side frame spring and friction wedge), side frame bogie, bearing adapter and wheelset (Fig. 6) are the components in MBS (Fig. 7). The mass of each component in this MBS will move relatively influenced by gravity g and the track provides a disturbing force f(x) that measured by Track Measuring Train (Fig. 5) on the track between Prabumulih Station to Kotabumi Station. The relative movement assumed according to the standard components contained in the software template.

Fig. 5. Track Measuring Train

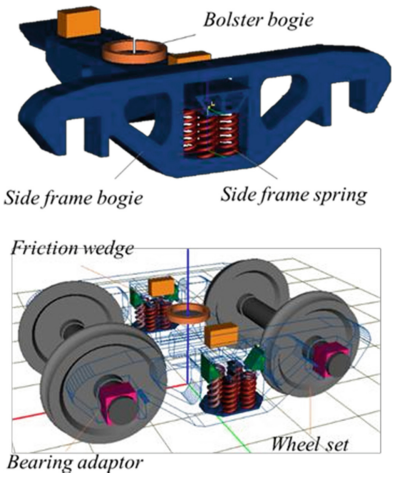

Fig. 6. The modelling of bogie set.

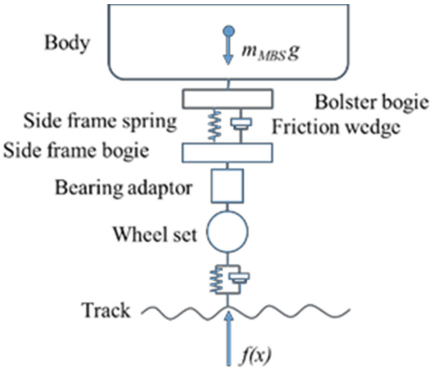

Fig. 7. Multi body system (MBS).

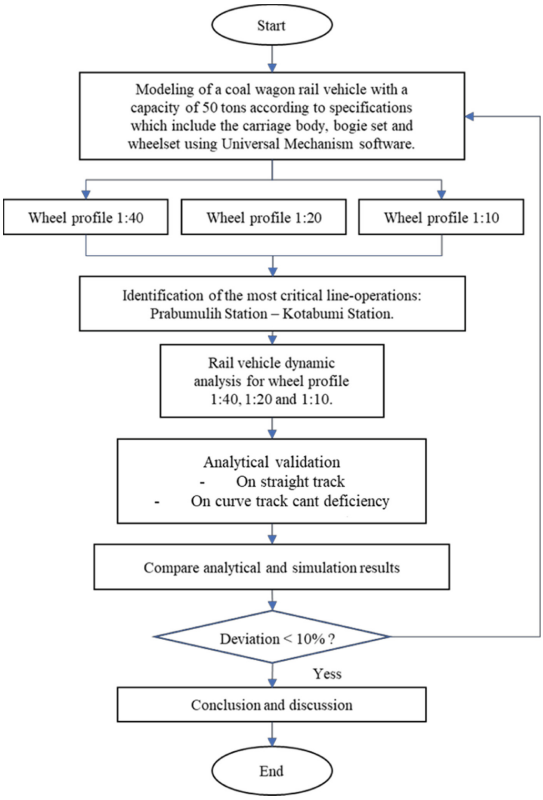

Fig. 8. Research flowchart.

The MBS is simulated to vary at 1:40, 1:20 and 1:10 wheel profile and the disturbing force of the track between Prabumulih Station to Kotabumi Station as f(x). The result of simulation to be validated by analytical method on both of the straight and curves track. Simulation and analytical results are compared and deviations are identified. Deviations that exceed 10% must recheck the modeling. The research flowchart is shown in Fig. 8.

2.3 Modeling Validation

Modeling is validated by analytical methods. Wagon specification data on Table 1 is used as input for calculations on straight and curve tracks.

In reality, the components that make up a rail vehicle system do not have a symmetrical center of gravity (COG), but are eccentric. In Indonesian railways, the COG eccentricity tolerance is 4%.

In this study, validation was carried out by comparing modeling simulations with analytical calculations using actual wagon specification data. From Fig. 9, the vertical axle force on the bogie MB (right side in Fig. 9) $W_{o,MB}$ is:

$$Wo, MB = \frac{1}{4} mkg \left(1 + \frac{xcg}{\frac{BB}{2}}\right) \tag{2}$$

Table 1. Wagon specification data.

Parameter	Value	Unit
mEmpty	13 000	kg
mLoaded	63 000	kg
mBogie		
mSideFrame	666	kg
mBolster	596.2	kg
mFrictionWedge	86.4	kg
mWSofMB	1 115	kg
mWSofTB	1 115	kg
xcog_wagon	173.74	mm
ycog_wagon	21.34	mm
zcog_wagon	1 039.00	mm
2x Semi Base (G)	1120	mm
BogieBase (BB)	10 830	mm
WheelBase (WB)	1 676	mm

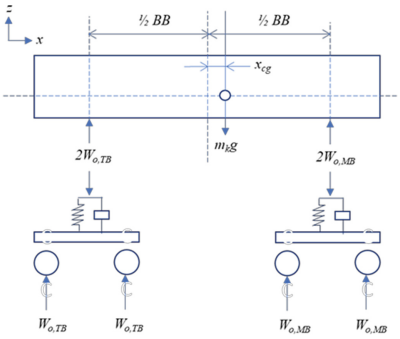

Fig. 9. Free Body Diagram (FBD) in the x-z plane.

where *mk* is the mass of the wagon, *g* is the acceleration due to gravity, *BB* is the bogie base, namely the distance between the center points of the bogies, and *xcg* is the center of gravity of the rail vehicle in the *x*-axis direction. The vertical axle force on the bogie TB, *Wo.TB* (left side in Fig. 9) is:

$$Wo.TB = \frac{1}{4}mkg\left(1 - \frac{xcg}{BB/2)}\right) \tag{3}$$

Figure 10 shows the forces acting on the rail vehicle in the y-z plane on straight track. Where ycg is the center of mass of the rail vehicle in the y direction and G is the

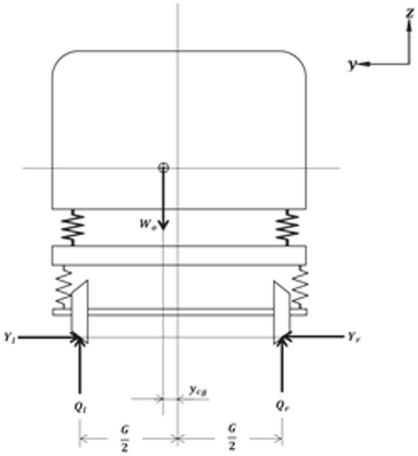

Fig. 10. FBD of y-z plane on straight.

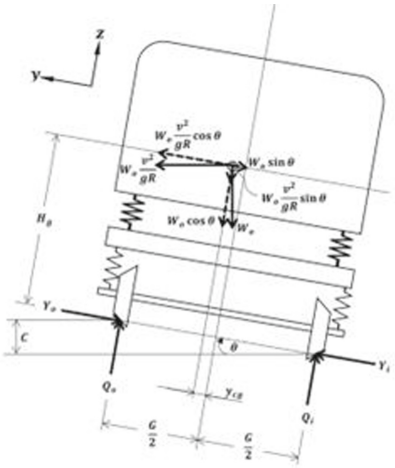

Fig. 11. FBD of y-z plane on curve.

contact point distance between the wheel surface and the rail, left and right. From the FBD, the vertical force on the left wheel (Ql) as:

$$Ql = \frac{Wo}{2}\left(1 + \frac{ycg}{\frac{G}{2}}\right) \tag{4}$$

Vertical force on the right wheel (Qr):

$$Qr = \frac{Wo}{2}\left(1 + \frac{ycg}{\frac{G}{2}}\right) \tag{5}$$

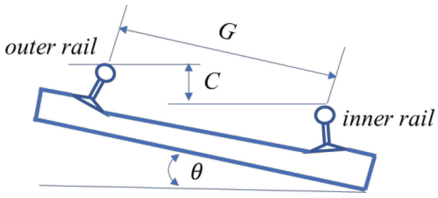

Fig. 12. Superelevation track on curve.

Table 2. Total gap analysis and simulation.

No.	Value	Gap
1	Vertical forces on straight track	5.56%
2	Vertical forces on curve track cant deficiency	4.38%
Total gap average		4.97%

Model validation was also carried out on rail vehicles while on curved tracks with FBD shown in Fig. 11. Rail vehicles passing through curves will cause centrifugal force. Excessive centrifugal force has the potential to cause the rail vehicle to roll outside the curve. So that on the outer rail a superelevation rail is made with a height of C, the angle of inclination is ɵ and the distance between the contact points of the left and right wheels with the rail is G (Fig. 12).

The forces acting on rail vehicles such as FBD in Fig. 11, are obtained by an analytical equation to determine the vertical force of the wheels on a curved trajectory. If *Qo* is the vertical force of the outer wheels, *Qi* is the vertical force of the inner wheels, *Wo* is vertical axle force, *ycg* is COG in *y*-axis direction, *R* is the radius of the curved rail, *v* is velocity of rail vehicle on curve, *Hg* is the height of the wagon's center of gravity in the *z*-axis direction, *C* is the elevation of the rail in the curve and *g* is gravitational acceleration. Validation will be calculation in the cant deficiency condition, where is $Qo > Qi$. So that on the outer wheel the vertical force *(Qo)* follows the equation:

$$Qo = \frac{Wo}{2}\left\{\left(1 - \frac{ycg}{\frac{G}{2}}\right)\left(1 + \frac{V^2 C}{gRG}\right) - \frac{Hg}{\frac{G}{2}}\left(\frac{V^2}{gR}\frac{C}{G}\right)\right\} \tag{6}$$

And the vertical force of the inner wheel *(Qi)*

$$Qi = \frac{Wo}{2}\left\{\left(1 - \frac{ycg}{\frac{G}{2}}\right)\left(1 + \frac{V^2 C}{gRG}\right) - \frac{Hg}{\frac{G}{2}}\left(\frac{V^2}{gR}\frac{C}{G}\right)\right\} \tag{7}$$

Analytical calculations using carriage specifications as input data and calculating the forces acting on straight and curved tracks using Eqs. (2)–(7) and the result is a gap of 4.97% as shown in Table 2. With this gap, the modeling simulation results are still relevant to use.

3 Result and Discussion

Data collection from modeling simulation using Universal Mechanism software was carried out after the model validation process was considered feasible or the value was below 10% (4.97%). This is important considering the actual conditions have been added to the safety factor value. So for example the derailment coefficient (Y/Q) has a ratio of 0.3, this means that in actual conditions, the (Y/Q) ratio can reach 0.75, that is, with a factor of safety of 2.5. That is, just 0.05 less to reach Nadal's derailment limit criterion, 0.8. The Rail Vehicle Dynamic Analysis simulation results at 1:40, 1:20 and 1:10 wheel profile show that the ratio (Y/Q) decreases as the speed increases.

3.1 Derailment Coefficient

Figure 13 shows the maximum (Y/Q) ratio at a speed of 10 km/h, at 1:40 the wheel profile is 0.357 (a). Whereas at 1:20 wheel profile is 0.292 (b) and 1:10 wheel profile is 0.226 (c). In Fig. 14, at speed of 35 km/h, at 1:40 the wheel profile drops to 0.342 (a). Whereas at 1:20 wheel profile drops to 0.287 (b) and 1:10 wheel profile to 0.200 (c). in Fig. 15, at speed of 60 km/h, the ratio (Y/Q) gets more smaller. In 1:40 the wheel profile is 0.335 (a), while in 1:20 the wheel profile is 0.263 (b) and 1:10 wheel profile is 0.187 (c).

From Fig. 13, it can be seen that the maximum (Y/Q) ratio occurs at the wheel-1R (axle 1-right). This indicates that most likely the derailment that occurred was in the cant excess condition. Where the derailment wheelset falls towards the curve. It can also be seen that the wheels-3R (axle 3-right) showed the second highest (Y/Q) ratio (0.329 at 10 km/h, 0.291 at 35 km/h and 0.225 at 60 km/h).

From Fig. 14, it still looks the same, where the 1R wheel dominates the highest (Y/Q) ratio followed by second place on the 3R wheel. The ratio (Y/Q) for all wheel profiles has decreased. The graph showing stable conditions can be seen in the 1:10 wheel profile where each wheel shows the ratio (Y/Q) with a small different.

In Fig. 15, shows the ratio graph (Y/Q) of wheels-1L which looks like overshadowing the ratio graph (Y/Q) of wheels-1R. This means, the rail vehicle is looking for its equilibrium point on the curve. Cant excess conditions can change to Cant deficiency even though it is still at a high (Y/Q) ratio. This also means that it is possible to have a 1:40 wheel profile derailment at a speed of 60 km/h in a radius of 350 m in cant deficiency.

Table 2 shows a recap of the simulation results of the 1:40, 1:20 and 1:10 wheel profiles at different speeds. It can be seen that the 1:20 wheel profile has 18.59% lower potential derailment than the 1:40 wheel profile. The 1:10 wheel profile shows an even greater reduction in potential derailment than the 1:40 wheel profile, which is 40.80% (Table 3).

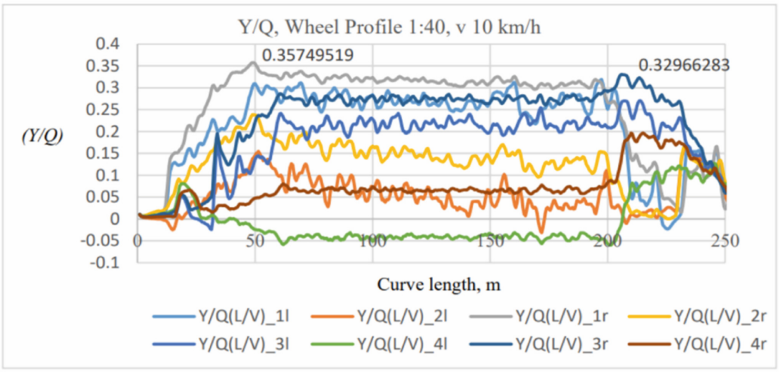

(a)

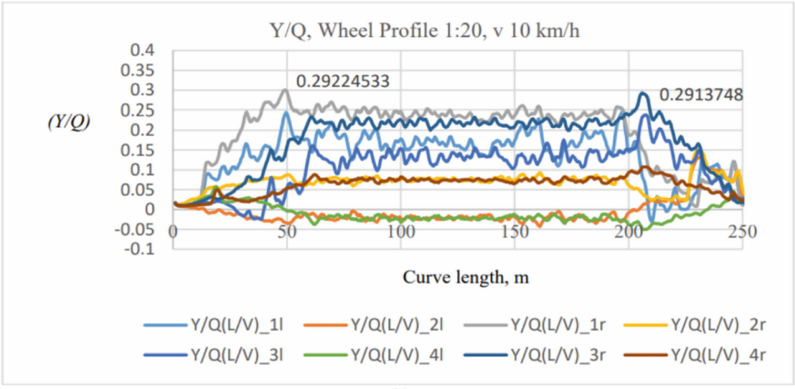

(b)

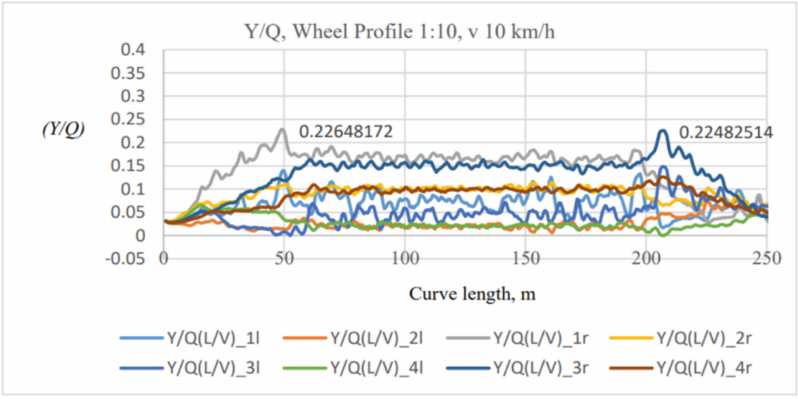

(c)

Fig. 13. Derailment coefficient (Y/Q) at radius curve 350 m and 10 km/h

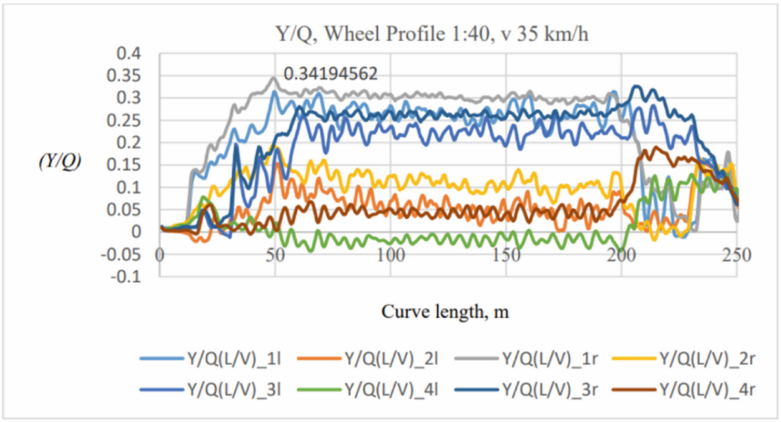

(a)

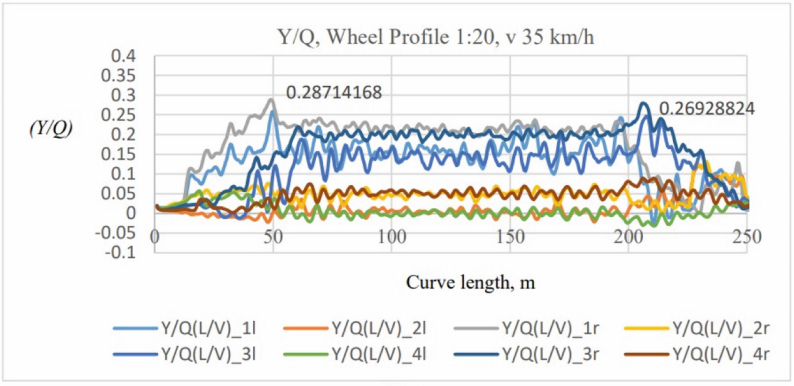

(b)

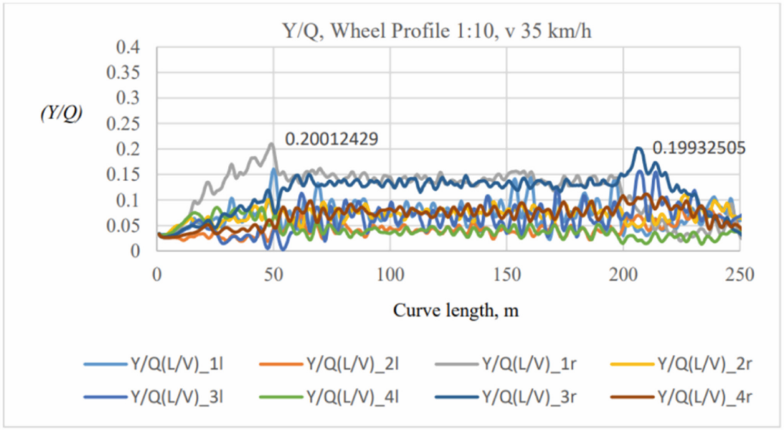

(c)

Fig. 14. Derailment coefficient (Y/Q) at radius curve 350 m and 35 km/h.

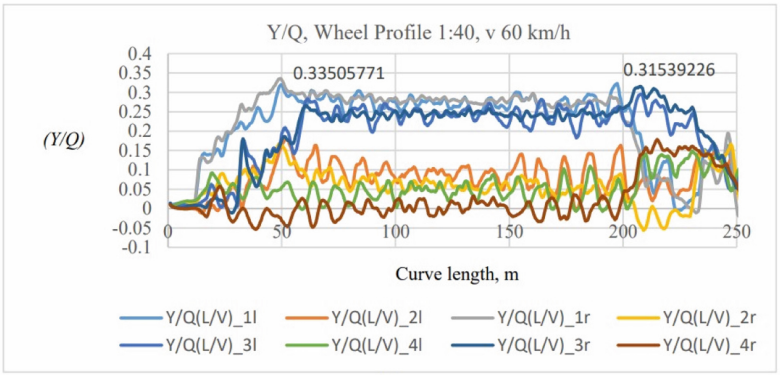

(a)

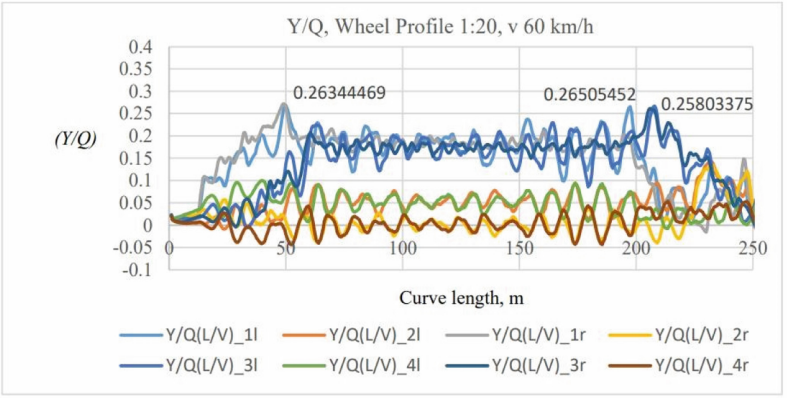

(b)

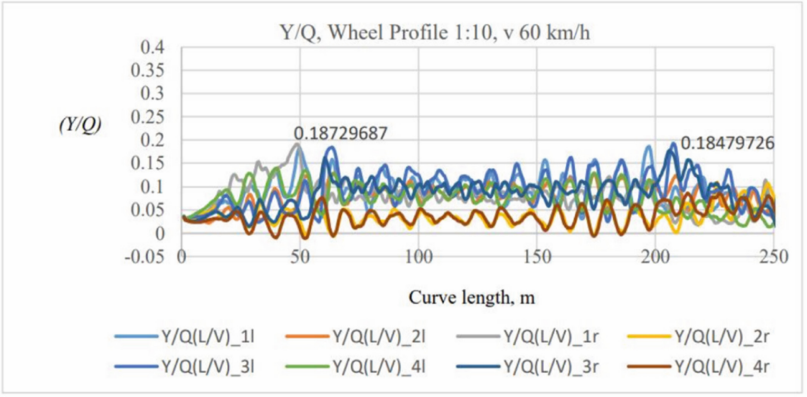

(c)

Fig. 15. Derailment coefficient (Y/Q) of 1:10 wheel profile at radius curve 350 m and 60 km/h.

Table 3. (Y/Q) Derailment coefficient of 1:40, 1:20 and 1:10 wheel profiles.

No.	V, Km/h	P40	P20	P10	P20/P40	P10/P40
1	10	0.357	0.292	0.226	81.79%	63.31%
2	35	0.342	0.287	0.200	83.92%	58.48%
3	60	0.335	0.263	0.187	78.51%	55.82%
				Average	81.41%	59.20%
				Reduction	18.59%	40.80%

Where: P40 = 1:40 wheel profile, P20 = 1:20 wheel profile, P10 = 1:10 wheel profile

4 Conclusion

Following are the things that can be concluded from this research:

1. Derailment coefficient. Wheel profiles with low conicity, such as 1:40 wheel profiles, show high derailment coefficient (Y/Q) ratio. On the other hand, a more conical wheel profile (1:20 and 1:10) indicates a lower (Y/Q) ratio. The 1:20 wheel profile shows 18.59% lower potential for derailment than 1:40 wheel profile and 1:10 wheel profile 40.80% lower;
2. The use of a more conical wheel profile (1:20 or 1:10) is recommended for use on the wheels of the Babaranjang train cars which operate on tracks with many curves and with a small radius such as in South Sumatra, especially between Prabumulih Station to Kotabumi Station to reduce the potential for derailment;
3. The general conclusion is that the proposed use of 1:20 or 1:10 wheel profiles on the 50-tons capacity wagon of the Babaranjang Train in South Sumatra, can be considered to replace the existing 1:40 wheel profiles, to reduce the potential for derailments that cause financial losses.

Acknowledgments. The authors want to thank for member of Riset Tim MAM Departemen Teknik Mesin dan Industri UniversitasGadjah Mada for any support.

References

1. I.Y. Shevtsov, Wheel/Rail Interface Optimisation (2008).
2. K. Knothe dan S. Stichel, *Rail vehicle dynamics* (2022).
3. J. Santamaria, J. Herreros, E.G. Vadillo, dan N. Correa, Veh. Syst. Dyn. **51**, 54 (2013).
4. A.C. Pires, L.A. Pacheco, I.L. Dalvi, C.S. Endlich, J.C. Queiroz, F.A. Antoniolli, dan G.F.M. Santos, Wear **477**, 203799 (2021).
5. S. Iwnicki, Handbook of Railway Vehicle Dynamics 2nd Edition 2019 (2019).
6. E. Butini, L. Marini, M. Meacci, E. Meli, A. Rindi, X.J. Zhao, dan W.J. Wang, Wear **436–437**, 203025 (2019).